Biexcitons in π-conjugated oligomers: Intensity-dependent femtosecond transient-absorption study

V. I. Klimov and D. W. McBranch
Chemical Science and Technology Division, CST-6, Mail Stop J585, Los Alamos National Laboratory, Los Alamos, New Mexico 87545

N. Barashkov and J. Ferraris
Chemistry Department, University of Texas, Dallas, Texas 75083

(Received 16 March 1998)

We report femtosecond transient-absorption (TA) studies of a five-ring oligomer of poly(*para*-phenylene vinylene) prepared in two different forms: solid-state films and dilute solutions. At high pump fluences, in both types of samples, we observe generation of two-exciton states, which are detected by the evolution of TA spectra and dynamics with increasing pump intensity. In solutions, double excitation of molecules results in the formation of stable biexcitons with enhanced oscillator strength, leading to an increased efficiency of the radiative decay and a superlinear pump dependence of the stimulated emission. In solid-state samples, the two-exciton states are unstable and decay on the subpicosecond time scale due to ultrafast charge transfer, accompanied by generation of interchain excitons. [S0163-1829(98)03336-0]

I. INTRODUCTION

Light-emitting polymers such as poly(*para*-phenylene vinylene) (PPV) have been intensively studied recently (for a review see, e.g., Ref. 1). The electronic and optical properties of these materials such as the energy gap and the emission wavelength can be tailored over a wide range by relatively simple chemical modifications of the molecular structure. Despite numerous investigations into the photophysics of π-conjugated polymeric systems, the nature and mechanisms of formation of the primary photoexcitations in these materials remain a matter of substantial controversy.[1–13] It is widely accepted that in dilute solutions with weakly interacting molecules, the dominant excitations are intrachain singlet excitons that have been described either as Coulombically bound electron-hole pairs[14,15] or self-localized ''polaron excitons.'' [16,17] In solid-state samples with strong intermolecular interactions, ultrafast charge transfer can lead to the formation of nonemissive interchain species, sometimes referred to as ''indirect excitons'' or bound polaron pairs.[5–9] These species have been cited by some authors as primary excitations in solid-state samples,[6–8] although this point of view is not universally accepted.[3,10,18]

Another issue that has been actively debated recently is the existence of coherent many-particle states such as cooperatively emitting excitons[19] and biexcitons.[20–29] Biexcitons have been extensively studied in inorganic semiconductors.[30–32] They were initially detected experimentally in wide-gap materials, such as CdS and CuCl by their signatures in photoluminescence (PL) spectra.[33,34] One of the effects associated with the formation of biexcitons is the enhancement of the oscillator strength of the exciton-biexciton transition due to coherent interactions of two excitons;[31] this is analogous to the effect of giant oscillator strength observed for excitons weakly bound to an impurity.[35] The observation of excitons in inorganic semiconductors is hindered by their small binding energies, which are typically in the range of several meV. Theoretical calculations show that the biexciton binding energy can be enhanced in quantum confined systems,[36] which has been confirmed experimentally by measurements of semiconductor quantum-dot structures.[37] Several theoretical papers have suggested the existence of biexcitons in organic π-conjugated systems,[21–24,28] but clear experimental verification of biexcitons as a general feature in these materials is still lacking. Multiexciton states have been observed in organic charge-transfer crystals.[20] The superlinear growth of stimulated emission at high intensities in luminescent conjugated polymers has been attributed to cooperative emission, possibly due to biexcitons.[19,26,29] However, there is now widespread agreement that this effect is due solely to amplified spontaneous emission.[38] A short-lived photoinduced absorption feature in a thiophene oligomer has been attributed to an ''intermolecular biexciton state,'' but without any systematic investigation of its dynamics and intensity dependence.[27] Hence it remains unclear under what conditions biexcitons are created, what their effects are on nonlinear absorption, and whether the properties of biexcitons in organic systems are similar to those in inorganic semiconductors.

In the present paper, we apply methods of femtosecond transient absorption (TA) to provide an experimental demonstration of the existence of stable biexcitons in π-conjugated molecules. To evaluate the role of intermolecular interactions at high excitation densities, we study two different forms of the same material: dilute solutions and solid-state films. We demonstrate that in solutions, at low pump densities, both the stimulated emission (SE) and the photoinduced absorption (PA) can be explained in terms of the generation of a single species: intrachain singlet excitons. With increasing pump intensity, the TA of solution samples clearly exhibits signatures of interaction between photoexcitations occupying a single chain, which we attribute to the formation

of stable biexcitons with oscillator strength enhanced due to the coherent interaction of two excitons. We also observe biexciton signatures in films. However, due to strong intermolecular interactions, two-exciton states in films are unstable and decay on the subpicosecond time scale with the formation of inter chain species.

II. EXPERIMENT

As a model system for our studies we have selected a five-ring PPV oligomer 2-methoxy-5-(2′-ethylhexyloxy) -distyryl benzene (MEH-DSB) [see Fig. 1(a), inset]. MEH-DSB can be prepared as high-quality thin films by vacuum sublimation and is also soluble.[39] Investigation of a model oligomer system allows us to avoid the effects of inhomogeneous broadening resulting from a distribution of conjugation lengths that are always present in amorphous polymer films. These distributions can lead to associated ultrafast ''random-walk'' energy relaxation dynamics[2] that complicate the interpretation of experimental data on subpicosecond time scales. MEH-DSB was prepared and purified as described in Ref. 40. Solutions were prepared using *p*-xylenes as a solvent. Amorphous thin films ($\sim$100 nm thickness) were deposited by vacuum sublimation onto sapphire substrates and transferred into an optical cryostat in a dry box to minimize the effects of photo-oxidation. As several authors have discussed,[13,40–42] the similarities in the optical and electronic properties of conjugated oligomers and polymers suggest that the results reported below are of general importance also for conjugated polymers.

TA studies were performed using a femtosecond pump-probe experiment. The samples were excited at 3.1 eV using 100-fs frequency-doubled pulses from a regeneratively amplified mode-locked Ti-sapphire laser (Clark-MXR CPA-1000). The pump-photon energy slightly exceeds the energy of the π-π^* transition in MEH-DSB ($\sim$2.9 eV), corresponding to near-resonant band-edge excitation. The transmission of the excited sample is probed by delayed pulses of a femtosecond continuum generated in a 1-mm-thick sapphire plate using $\approx 2\ \mu$J of the fundamental beam at 800 nm. The reported spectra have gaps near the fundamental wavelength due to strong variations of probe intensity near 800 nm. As a measure of transmission changes we use the differential transmission (DT), defined as $DT=(T-T_0)/T_0 = \Delta T/T_0$, where T_0 and T are transmissions in the absence and in the presence of the pump, respectively. In the case of negligibly small resonator effects, DT can be transformed into a pump-induced absorption change ($\Delta\alpha$) using the relationship $\Delta\alpha = -(1/d)\ln(1+DT)$ (d is the sample thickness). In the small signal limit ($DT \ll 1$), $\Delta\alpha$ is simply proportional to DT: $\Delta\alpha \approx -DT/d$.

Time-resolved DT data were obtained in two different experimental configurations. DT spectra at a fixed delay time Δt between pump and probe pulses were recorded with a 0.15-m spectrometer coupled to a liquid-nitrogen-cooled charge coupled device camera by averaging the signal over 1000–2000 pulses. This type of measurement provides information on the spectral distribution of the nonlinear optical response over a broad spectral range (0.45–1.1 μm) with an accuracy up to 10^{-3} in DT. In the other configuration, DT spectra and single-wavelength DT dynamics were monitored with much higher accuracy (up to 10^{-5} in DT) using phase-sensitive detection with a lock-in amplifier synchronized to a chopped pump beam. In addition to the improved sensitivity, the above method can be used for recording chirp-free TA spectra by scanning the monochromator and simultaneously adjusting the relative pump-probe delay according to the calibrated chirp.[43]

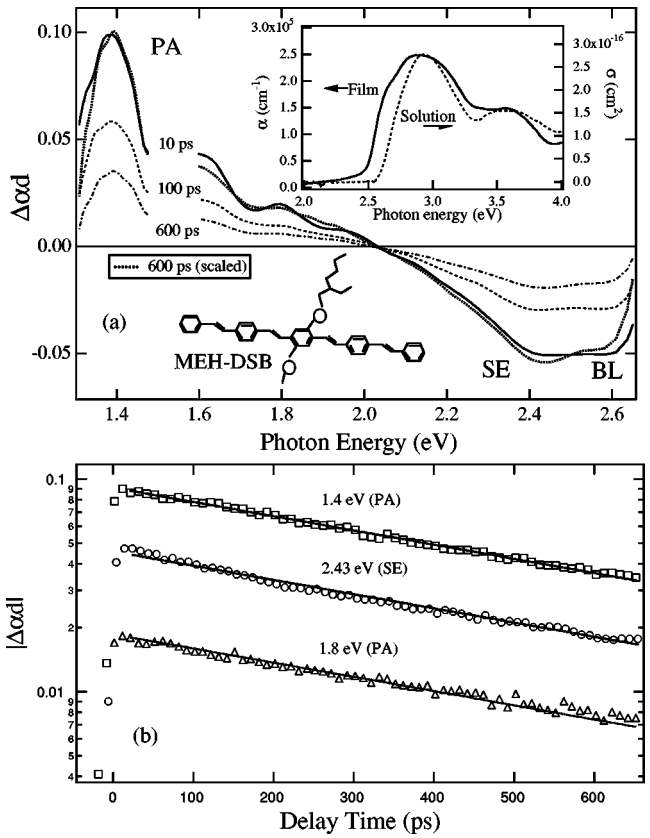

FIG. 1. (a) TA spectra for MEH-DSB in solution recorded at $w_p = 0.08$ mJ cm^{-2} for different delay times Δt between pump and probe pulses (indicated in the figure). The scaled 600-ps spectrum (dotted line) is nearly identical to the spectrum taken at $\Delta t = 10$ ps (solid line), indicating that the TA decay is spectrally uniform. Inset: the absorption coefficient of MEH-DSB film (solid line) and absorption cross section of MEH-DSB in solution (dotted line). (b) Dynamics of SE (1.4 eV) and PA (1.4 and 1.8 eV) in the sample fit to an exponential decay with a time constant of 650 ps. The 2.6-eV negative TA peak is labeled BL, for ''bleach'' (see the text).

III. EXCITON AND BIEXCITON DYNAMICS FOR ISOLATED MOLECULES (DILUTE SOLUTIONS)

A. Transient absorption of MEH-DSB solutions

Figure 1 displays time-resolved spectra of absorption changes of the MEH-DSB solution sample recorded in the low-pump-intensity regime at a pump fluence $w_p = 0.08$ mJ cm^{-2}. Given the absorption cross section at the pump wavelength $\sigma_p = 2.3\times10^{-16}$ cm^{-2} (derived from linear absorption data), this corresponds to the excitation of $N_{eh} \approx 0.04$ electron-hole pairs per molecule on average [$N_{eh} = \sigma_p(w_p/\hbar\omega_p)$, $\hbar\omega_p$ is the pump photon energy]. The DT spectra show a pronounced negative band (pump-induced bleaching) at high spectral energies (2–2.7 eV) and

a broad weakly structured positive band (PA) below 2 eV with a maximum at ~1.39 eV [see Fig. 1(a)]. The bleaching band shows two weakly pronounced maxima at 2.45 eV and 2.6 eV. The maximum at ~2.4 eV is located below the absorption edge, which suggests that it is due to SE in response to probe photons. This assignment is in agreement with TA data from Ref. 5 and the demonstration of efficient lasing in MEH-PPV solutions in Ref. 44. The 2.6-eV maximum occurs in the range of the onset of the strong absorption [see the absorption spectrum in the inset to Fig. 1(a)] and is likely dominated by pump-induced bleaching due to depopulation of the ground state; the contribution from SE at this wavelength is expected to be small, due the relatively large absorption and small luminescence. The absorption [see Fig. 1(a), inset] and emission spectra for solution and film are quite similar, other than the additional inhomogeneous broadening observed in the film. Hence the ground-state optical properties are not significantly affected by interchain effects (e.g., excimer formation).

In the low-pump-intensity regime, the TA decay is spectrally uniform, which is seen from the close match of the scaled 600-ps spectrum [dotted line in Fig. 1(a)] and the spectrum recorded at 10 ps after excitation [solid line in Fig. 1(a)]. The TA dynamics recorded at the SE maximum and at two different spectral energies within the PA band [Fig. 1(b)] show nearly identical exponential decay, with a time constant of 650 ± 50 ps. The spectrally uniform TA dynamics indicate that all TA features (PA and SE) are due to the same species. As these species are associated with the efficient SE, they can be assigned to intrachain singlet excitons, in agreement with previous measurements in MEH-PPV solutions.[8] The TA relaxation dynamics give a measure of the radiative lifetime of excitons in MEH-DSB: $\tau_r \approx 650$ ps, which is close to the reported values for MEH-PPV in solution (700 ps).[45]

At pump levels exceeding ~0.4 mJ cm^{-2}, both the PA and the SE dynamics start to deviate from a single exponential (Fig. 2). The high-intensity SE dynamics indicates the presence of an additional fast component [Fig. 2(a)], whereas the initial PA becomes slower at high excitation densities [Fig. 2(b)]. These opposite trends lead to increasing deviations between the PA and the SE relaxation dynamics with increasing pump intensity. A simple analysis of SE dynamics using a double-exponential fit shows that all time transients can be well described using two time constants 160 ± 25 ps (fast decay) and 650 ± 50 ps (slow decay), which are essentially the same for all pump intensities. Analyzing the correlation between amplitudes of the fast (A_f) and slow (A_s) components [see the inset to Fig. 2(a)], we arrive at the relationship $A_f \propto A_s^2$, which is indicative of two correlated components, contributing to the SE feature. Given the observed quadratic pump dependence of A_f, it is reasonable to infer that the fast SE component originates from doubly excited molecules (intrachain two-exciton states or biexcitons), which are generated during the pump laser pulse via sequential reexcitation of singly excited molecules. The fact that the lifetime of the biexciton is shorter than that of an exciton is indicative of strong interactions between excitations occupying a single chain, leading to the enhanced radiative decay. This effect has been previously observed in inorganic semiconductors and explained in terms of the enhancement of the

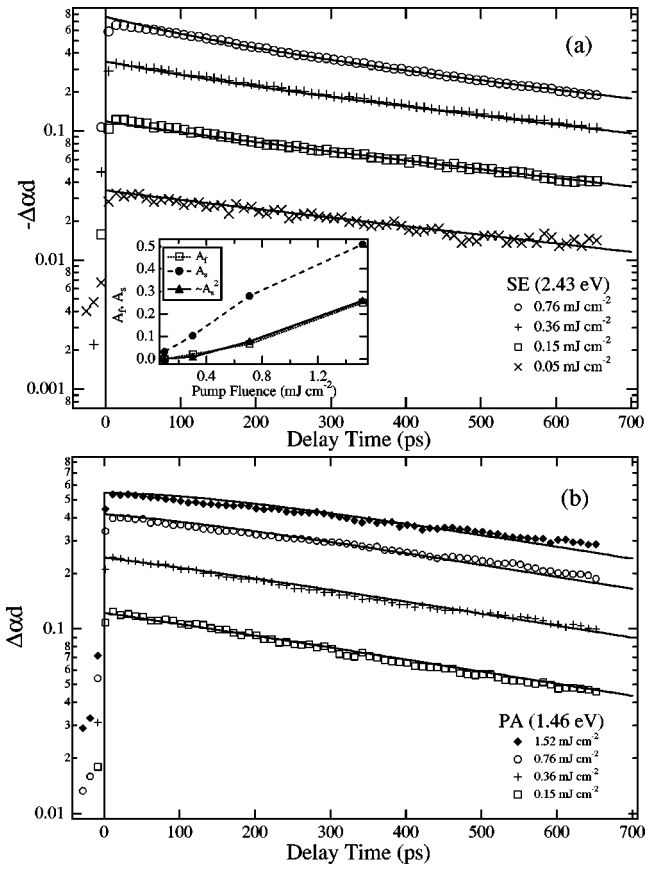

FIG. 2. Pump-intensity-dependent dynamics of (a) SE (2.43 eV) and (b) PA (1.46 eV). Symbols are measured data, while the fits to a model accounting for generation of singlet excitons and biexcitons are shown as lines (see the text for details of the model). The inset in (a) shows quadratic correlations between amplitudes of the fast (A_f) and slow (A_s) SE components derived from the double-exponential fits.

oscillator strength (f_{bx}) of the exciton-biexciton transition.[31] The enhancement factor $\beta = f_{bx}/f_x$ (f_x is the exciton oscillator strength) scales roughly as a ratio of the biexciton-to-exciton volumes, which can be understood in terms of the superradiant emission of two coherent oscillators[31] or coherent exciton-exciton interactions. Superlinear PL has been widely observed in PPV polymers;[19,29,46,47] there is now widespread agreement that this effect is due to line narrowing of amplified spontaneous emission.[38] In contrast, our $\Delta\alpha$ measurements contain no line-narrowing effect; the superlinear SE is therefore only due to an increase in the oscillator strength.

The difference in PA and SE dynamics in the high-pump-intensity regime can be explained by the fact that biexcitons contribute differently to SE and to PA. This is not surprising since the final states involved in these two processes are different. SE is associated with the *interband conduction to valence-band transition*, whereas PA is due to *intraband transitions* within the same band. The fact that the species generated at high intensities have a different effect on SE and PA is also clearly seen from the TA pump dependence recorded at 1.64 (PA) and 2.45 eV (SE) (see Fig. 3). At low pump fluences, the PA signal (1.64 eV) is greater than the SE signal (2.45 eV). With increasing pump intensity, PA grows

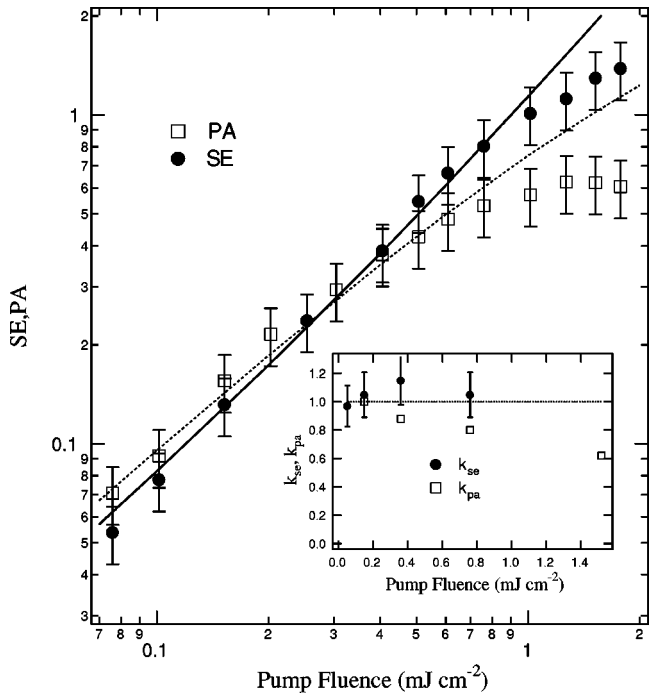

FIG. 3. Pump dependence of SE (2.43 eV) and PA (1.46 eV) signals (symbols) measured at 5 ps after excitation in comparison with modeling results (lines) obtained assuming that the ratio of the biexciton to the exciton contributions to the SE and PA are 4.5 and 0.5, respectively. Inset: pump dependence of the amplitude correction coefficients used to model SE and PA dynamics (see the text for details).

almost linearly with w_p, whereas SE shows a superlinear increase that leads to the intersection of the PA and SE pump dependence at around 0.4 mJ cm^{-2} (see Fig. 3). Above this threshold value, SE is greater than PA.

B. Modeling of transient absorption for solution samples

To analyze the high-intensity TA in more detail we have performed numerical modeling of the TA dynamics taking into account contributions from both excitons and biexcitons. To describe the generation of excitons, we use a pump rate $g(t)$ with a Gaussian temporal profile and a unit area, multiplied by a factor $1-n_x$ (n_x is the exciton density normalized by the total density of molecules n_0) that accounts for saturation of the exciton density in the limit $n_x \rightarrow 1$. In our model, the biexcitons are generated by a sequential reexcitation of singly excited molecules (excitons). The corresponding generation rate is $Bg(t)n_x$, where $B=0.85$ is determined experimentally as detailed below. We further assume that the exciton and biexciton decay is dominated by radiative processes with corresponding time constants τ_x and τ_{bx}. The ratio of these constants is determined by the enhancement factor β for the biexciton oscillator strength: $\tau_x/\tau_{bx}=\beta$. The radiative decay of the exciton leads to generation of a photon, whereas the biexciton decays into a photon and an exciton. Under the above assumptions, the rate equations for normalized exciton (n_x) and biexciton (n_{bx}) concentrations can be written as

$$\frac{dn_x}{dt}=w_n g_0 g(t)(1-n_x)-w_n B g_0 g(t) n_x-\frac{n_x}{\tau_x}+\frac{n_{bx}}{\tau_{bx}}, \tag{3.1}$$

$$\frac{dn_{bx}}{dt}=w_n B g_0 g(t) n_x-\frac{n_{bx}}{\tau_{bx}}, \tag{3.2}$$

where $w_n \leqslant 1$ is the pump fluence normalized by its maximum value used in the experiments with solution samples ($w_{max}=1.52$ mJ cm^{-2}) and g_0 is the magnitude of the maximum pump rate. The relative value of the biexciton generation rate B was determined from the population of excitons and the corresponding values of the photoinduced bleaching at the pump wavelength ($\Delta\alpha/\alpha$), using the expression

$$B=1-\frac{\Delta\alpha}{\alpha n_x}. \tag{3.3}$$

The SE signal was modeled as proportional to $n_x+\beta n_{bx}$, which accounts for the enhanced oscillator strength of the biexciton. The PA signal is assumed to be proportional to $n_x+\gamma n_{bx}$, where γ is the ratio of the biexciton to exciton absorption cross sections at the PA wavelength. In our modeling, we used the time constant $\tau_x=650$ ps derived from the measured TA dynamics at low intensity. The biexciton radiative time constant τ_{bx} is given by $\tau_{bx}=\tau_x/\beta$. From the double-exponential fits above, we estimate $\beta \approx 4$. The only adjustable parameters in the fitting procedure are β and g_0.

We first modeled the pump-dependent SE dynamics in Fig. 2(a) and the pump dependence of the peak SE (probe time delay 2 ps) in Fig. 3. The value of g_0 ($g_0=0.7$) was chosen to fit the SE time transient taken at the highest pump level in Fig. 2(a), where the superlinear SE is most evident, using $\beta=4$. β was then varied with g_0 fixed to obtain the best fits to the data in Figs. 2(a) and 3. Time transients taken at lower pump intensities are fit by using experimentally measured pump intensities w_n, without further adjustments in g_0. To achieve a closer match between calculated and measured SE amplitudes, the computed curves are multiplied by a correction factor k_s (Fig. 3, inset).

Using the above procedure, we obtained excellent fits to the SE dynamics over a pump range from 0.05 to 0.76 mJ cm^{-2} [see Fig. 2(a)]. Our model also provides a good fit to the pump-dependent SE amplitudes (Fig. 3). As seen from the inset to Fig. 3, over the pump-intensity range studied, the amplitude correction factor varies by less than $\pm 15\%$. From this modeling, we conclude that $\beta=4.5 \pm 0.5$.

To fit the pump-dependent PA time transients, we used the parameter g_0 derived from the SE fits, so that only one adjustable parameter γ was used. The fit to the PA trace recorded at the highest pump intensity in Fig. 2(b) yields $\gamma=0.4\pm0.05$, indicating that PA is dominated by the exciton contribution ($\sigma_x/\sigma_{bx}=2.5$). This value of γ is further used to fit the traces recorded at lower pump levels. To adjust the amplitudes of the computed PA curves we introduce the pump-dependent correction factor k_p. As seen in Fig. 3, this procedure leads to a systematic overestimation of the PA, necessitating a monotonic reduction in k_p in order to match the absolute magnitude of the PA.

As seen from the fits in Fig. 2(b), the above simple model allows us to understand the principal trends in the pump-dependent PA dynamics. The model predicts correctly the slowing down in the initial PA decay at high pump intensities and the characteristic negative curvature of the early

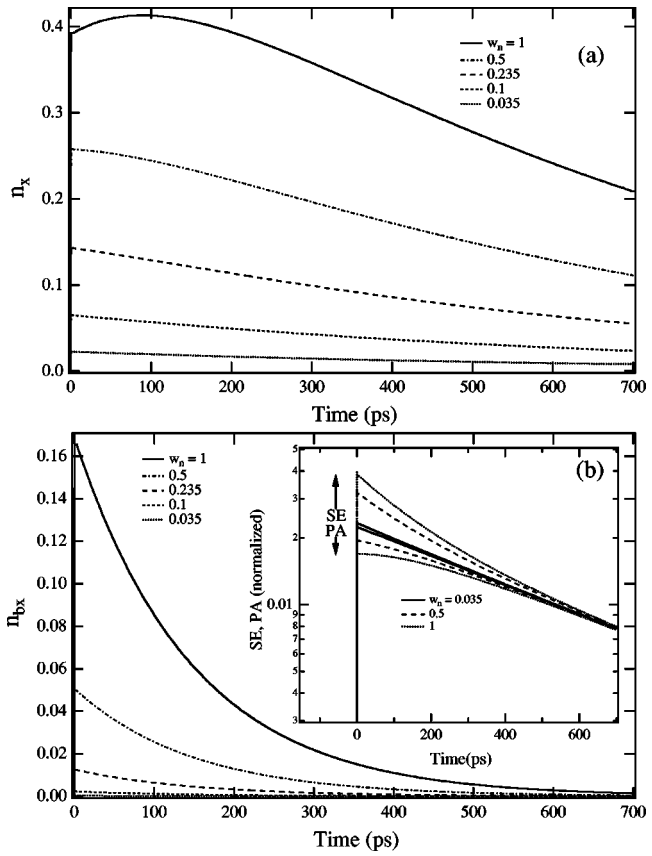

FIG. 4. Results of the modeling for the (a) pump intensity-dependent exciton and (b) biexciton dynamics. The inset in (b) shows the calculated SE and PA dynamics (as in Fig. 2), normalized to the signal population at long times, to highlight the opposite trends in intensity-dependent dynamics for SE (upper series) and PA (lower series)

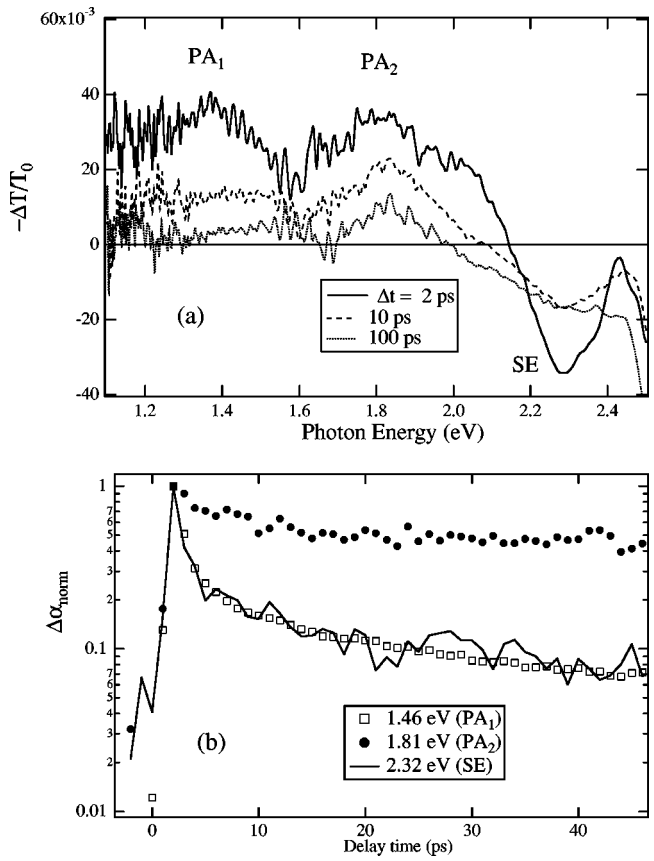

FIG. 5. (a) Two PA features (PA_1 and PA_2) in the time-resolved DT spectra of the MEH-DSB film ($w_p = 2.5$ mJ cm^{-2}). (b) Matching dynamics of the SE (2.32 eV) and PA_1 (1.46 eV) features along with distinct dynamics of the PA_2 feature (1.81 eV).

time-dependent PA signal. The fit to the PA amplitudes is somewhat worse than for the SE signal. With increasing pump level, the correction parameter k_p monotonically decreases from 1 to around 0.6. This is a reflection of the saturation of the measured PA signal above ~ 0.8 mJ cm^{-2} (see Fig. 3). This saturation is not predicted by the model and occurs probably due to saturation of absorption at the pump wavelength and/or higher-order effects, such as generation of triply excited molecules.

The strongest point of the model is that the same set of parameters derived by fitting the time transients allows an excellent fit of the pump dependence the PA and SE as seen from Fig. 3 (lines). The model describes well both the slopes of the SE and PA pump dependence and the crossing in pump-dependent SE and PA amplitudes at around 0.4 mJ cm^{-2}.

A deeper insight into the TA transient behavior is provided by analysis of the calculated pump-dependent exciton and biexciton dynamics (see Fig. 4). At low pump intensities ($n_x < 0.1$), the ratio of concentrations of doubly to singly excited molecules is below 10%. Since the biexciton concentration scales approximately as the square of the pump fluence, this ratio grows with increasing pump intensity; for $n_x \approx 0.4$ it exceeds 40%. The generation of biexcitons has a significant effect on the exciton dynamics, leading to the slowed decay and the delay of the peak exciton population [see Fig. 4(a)], which is due to regeneration of excitons during the biexciton decay. Since PA is dominated by the exciton contribution, this behavior transfers to the PA dynamics, leading to the slowing down of the PA relaxation in the high-intensity regime. Due to the enhanced biexciton oscillator strength, the SE at high pump levels is dominated by biexcitons, which results in the increased amplitude of the biexciton-related fast component in the SE signal. These opposite trends in the PA and SE pump dependence lead to the increasing deviation in their dynamics at high pump intensities [inset to Fig. 4(b)], as also seen from the experimental time transients (Fig. 2). Interestingly, our simple model provides a very accurate description of the absolute carrier densities generated in the material. For example, the estimate of the carrier density at a pump fluence of $w_n = 0.5$ yields $N_{eh} = 0.35$. This is in close agreement with the computed value of 0.34, determined as $n_x + 2n_{bx}$ [see modeling results in Figs. 4(a) and 4(b)].

Since our measurements were limited to a single-length oligomer, we cannot yet determine whether the observation of biexcitons in short-length π-conjugated systems is facilitated by spatial confinement. However, theoretical and experimental data available for inorganic semiconductors indicate a crucial role of quantum confinement in the stabilization of two-exciton states.[36,37]

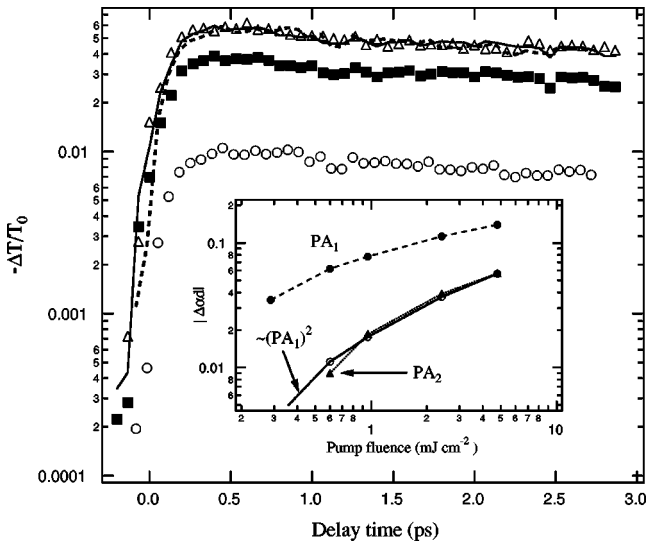

FIG. 6. Time transients demonstrating pump-independent dynamics of the PA_2 feature, for $w_p = 6\ \mathrm{mJ\ cm^{-2}}$ (open triangles), $3\ \mathrm{mJ\ cm^{-2}}$ (solid squares), and $0.6\ \mathrm{mJ\ cm^{-2}}$ (open circles). Solid and dashed lines are data taken at 3 and 0.6 $\mathrm{mJ\ cm^{-2}}$, respectively, scaled to the 6-$\mathrm{mJ\ cm^{-2}}$ data. Inset: PA pump dependence indicating a quadratic correlation $[PA_2 \sim (PA_1)^2]$ in the peak magnitudes of the PA_1 and PA_2 features.

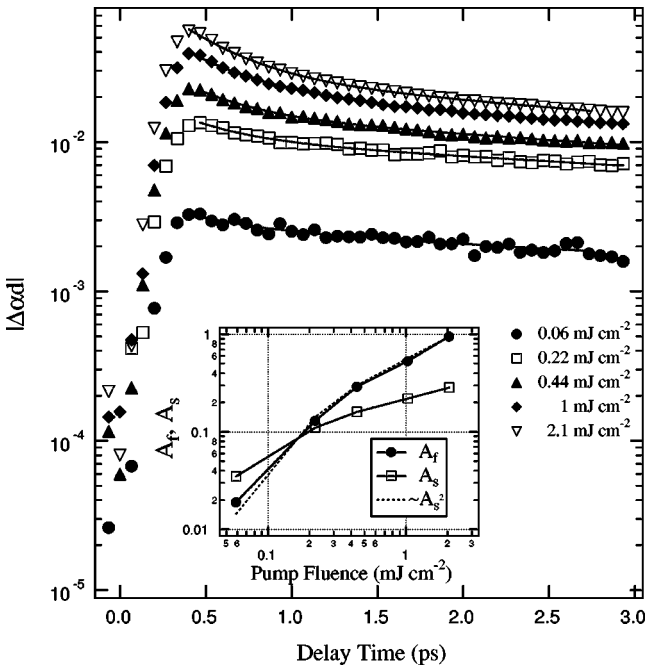

FIG. 7. Pump-intensity-dependent time transients of PA_1 feature at 1.46 eV (symbols) plotted together with double-exponential fits (lines). Data are shown for $w_p = 2.1\ \mathrm{mJ\ cm^{-2}}$ (open triangles), $1\ \mathrm{mJ\ cm^{-2}}$ (solid diamonds), $0.44\ \mathrm{mJ\ cm^{-2}}$ (solid triangles), $0.22\ \mathrm{mJ\ cm^{-2}}$ (open squares), and $0.06\ \mathrm{mJ\ cm^{-2}}$ (solid circles). Inset: quadratic correlation in the pump dependence of the magnitudes derived for the fast (A_f) and the slow (A_s) components from the double-exponential fits $[A_f \sim (A_s)^2]$.

IV. EXCITONS AND BIEXCITONS IN SOLID-STATE FILMS

A. Transient absorption of film samples

In Fig. 5 we show time-resolved DT spectra [Fig. 5(a)] and single-wavelength DT time transients [Fig. 5(b)] recorded for the MEH-DSB film. In contrast to solutions, which display relatively slow (subnanosecond) exponential DT dynamics, the DT decay in films is much faster (picosecond time scale) and is strongly nonexponential. We also see an increase of the PA signal at ~ 1.8 eV, indicative of the formation of a new short-wavelength PA band. The fact that two distinct spectral bands are present in solid-state samples is confirmed by an analysis of the DT dynamics at various wavelengths. The 1.4-eV band (PA_1) shows much faster decay than the feature at 1.8 eV (PA_2) [see Fig. 5(b)]. In addition to that, the dynamics of two PA features have markedly different pump dependence (Figs. 6 and 7). On the 3-ps time scale shown in Fig. 6, PA_2 exhibits *pump-independent* and almost exponential decay with an initial fast relaxation time constant of about 6 ps [note the overlap of the scaled time transient of the lower-intensity data (lines) and the higher-intensity data (open triangles) in Fig. 6]. In stark contrast, the dynamics of the PA_1 band are clearly nonexponential even at short delay times (see Fig. 7) and show *a pronounced pump-intensity dependence*, which will be discussed below.

The existence of two distinct PA bands with different dynamics in solid-state samples clearly indicates contributions from at least two different species to the TA. Although the PA_1 decay dynamics are intensity dependent, in pristine films they match very closely the SE dynamics over a wide pump-intensity range [see Fig. 5(b) and the data in Ref. 18]. This clearly shows that, as in solutions, the PA_1 feature arises from the same species as the SE, namely, from emissive intrachain singlet excitons.

The fact that we do not see any SE features associated with the PA_2 band indicates that this band might be related to the nonemissive interchain excitons predicted in Refs. 6–8. This explanation is consistent with the observed pump-independent dynamics (Fig. 6) that are expected for strongly correlated geminate electron-hole pairs located on closely separated chains.[6] Additional PA features may be expected for triplet excitons;[16] however, this explanation is not consistent with our data. Although singlet fusion could account for fast rise times of triplet excitons, we only observe the second PA band in solid-state samples and not in solutions. In addition, the short (picosecond) decay dynamics of this band are inconsistent with the long lifetime expected for triplet excitons.

To examine in more detail the pump-dependent dynamics of the PA_1 feature, we performed a double-exponential fit to the PA_1 time transients as shown in Fig. 7. As a result of this fit we find that both the initial fast and subsequent slow decay time constants are essentially *independent* of the pump fluence and are close to 450 fs and 6 ps, respectively. The apparent intensity-dependent decay on the shortest time scales results from an evolution of the *relative magnitudes* of these two decay components. The pump-intensity dependence of the amplitudes of the fast (A_f) and the slow (A_s) components is displayed in the inset to Fig. 7. As in solution samples, these data reveal the dependence $A_f \propto A_s^2$, which is indicative of generation of two-exciton states (biexcitons). However, in contrast to solutions where biexcitons are relatively long lived, two-exciton states in films decay on the sub-picosecond time scale, due to enhanced intermolecular

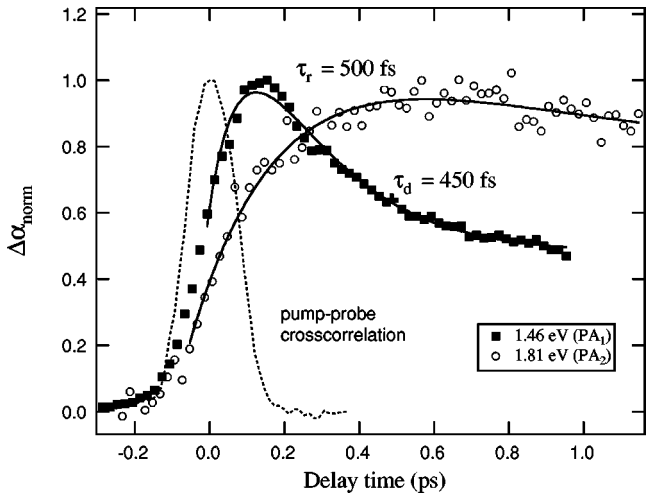

FIG. 8. Complementary subpicosecond dynamics recorded for the PA_1 and PA_2 features in the film, plotted together with the pump-probe cross correlation, which defines the temporal resolution of the experiment.

interactions. In dilute solutions with well-separated molecules, intermolecular interactions are suppressed and double excitation of molecules leads to the formation of stable relaxed biexcitons that decay primarily via radiative processes. In films with densely packed chains, strong intermolecular interactions facilitate the decay of doubly excited molecules due to an ultrafast charge transfer with the formation of interchain species (interchain excitons), responsible for the PA_2 band.

This mechanism for the biexciton decay is confirmed by an analysis of the short-term PA_1 and PA_2 dynamics (Fig. 8). The buildup of the PA_1 band is very fast and occurs essentially within the duration of the pump pulse. On the other hand, PA_2 shows a delayed buildup (time constant of about 500 fs) that is complementary to the initial fast relaxation of the PA_1 feature (time constant of about 450 fs) associated with the decay of the two-exciton states. These data are consistent with the scenario in which the charge-transfer species are generated at the expense of the doubly excited molecules, which can be considered as unrelaxed ''hot biexcitons.'' Additional support for our interpretation of the TA data is provided by the observation of a quadratic correlation in the pump dependence of the PA_1 and PA_2 features, evident from the data in the inset to Fig. 6. It is also important to mention that the PA_2 feature can only be observed at high pump intensities (above $\sim 0.6\ \mathrm{mJ\ cm^{-2}}$), for which the ratio of concentrations of doubly to singly excited molecules exceeds 10%.

We believe that our model allows the explanation of an important trend that has been observed for many phenylene-based conducting polymers and oligomers: The PL and SE efficiencies in solid-state films are often significantly reduced in comparison to the corresponding efficiencies in solutions.[1,8,10] Our measurements of SE pump dependence in MEH-DSB films and solutions show that at low pump levels the SE efficiency is comparable in these two types of samples. However, at higher pump levels, in the regime where significant numbers of molecules are doubly excited by a laser pulse, we see *a saturation of the SE in films* and *a superlinear SE growth* in solutions. We think that both effects have their origins in the generation of two-exciton states, but with a different outcome depending on the strength of intermolecular interactions. In solutions, double excitation of molecules leads to the formation of biexcitons with the associated enhancement of the oscillator strength, whereas in films, doubly excited molecules are the source for the formation of nonemissive interchain species, which leads to the reduction of SE and PL efficiency at high pump fluences.

B. Photodegradation in solid-state films

The interpretation of the ultrafast PA features in solid-state samples of PPV derivatives has been highly controversial.[48,1,3–13] In films of PPV,[6,7,48] methoxy-PPV,[5] MEH-PPV,[8] poly[2-butyl-5-(2'-ethyl-hexgl)-1,4-phenylene vinylene],[12] and a ladder-type poly(para-phenylene) derivative,[9] the SE and PA dynamics were observed to be different. Hence, for these materials it was concluded that the PA is entirely or partially due to species that are different from those responsible for the SE. However, correlations between the SE and PA decays have been reported for films of PPV,[4] poly (3-hexyl thiophene),[49] and poly(*p*-pyridyl vinylene).[11] We believe that the reason for many of the inconsistencies in previously published experimental data is the uncontrolled photo-oxidation of the samples, which has a strong effect on the TA dynamics.[1,10,13,48,50]

Our measurements show that irreversible photochemical changes take place in MEH-DSB films, even in an evacuated cryostat, under moderate pulsed excitation levels. Photochemical degradation is characterized by an overall reduction in the magnitude of DT and a dramatic change in the dynamics of the SE emission as detailed below. These effects were observed at per pulse excitation levels above $\sim 4-5\ \mathrm{mJ\ cm^{-2}}$ *and* when irradiating the films with a cumulative fluence (multiple pulses at a single spot on the sample) greater than $\sim 1\ \mathrm{kJ\ cm^{-2}}$. In photodegraded (photo-oxidized) samples, at pump intensities above $\sim 4\ \mathrm{mJ\ cm^{-2}}$ we observed that the SE dynamics no longer matched those of the PA_1 band [Fig. 9(a)]. The TA signal at 2.32 eV (SE maximum in pristine samples) rapidly switched from SE (positive DT) to PA (negative DT) [Fig. 9(a), solid circles], similarly to the crossover previously observed in PPV films,[7] where the difference in PA and SE dynamics was cited as evidence of a distinct species contributing to the near-IR PA band. Interestingly, by lowering the pump intensity we again return to the regime where PA and SE dynamics match each other [Fig. 9(b)], although the magnitude of the TA signal is then reduced by approximately a factor of 4 for both SE and PA.

Our observations can be explained within the following picture. Prolonged laser irradiation of sufficiently high intensity results in generation of defects via, e.g., loss of conjugation due to cleaving of the vinylene double bonds to form terminal carbonyl species as was previously suggested in Ref. 48. These defects contribute to TA by a PA signal that is likely spectrally overlapping with SE. However, the defect states cannot be photoexcited directly by incident photons, but rather only via a charge transfer mediated by intrachain excitons. As in the case of interchain excitons formation, the charge transfer is only efficient at high pump intensities in the regime where a large number of molecules are doubly

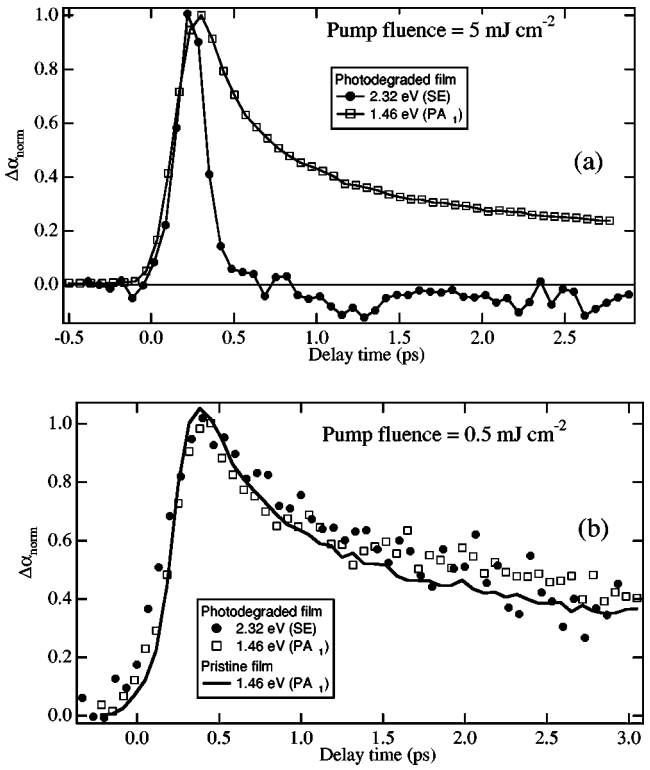

FIG. 9. Comparison of the SE and PA_1 dynamics in the photodegraded film at (a) high and (b) low pump fluences. In contrast to pristine films, the SE and PA_1 dynamics strongly deviate from each other at high pump levels.

excited. Therefore, at low pump fluences the SE dynamics are not significantly affected by the presence of defects. The main effect of photodegradation in this case is the overall reduction of the TA signal (PA and SE) due to reduced concentration of conjugated molecules, which also leads to the quenching of PL observed previously in photodegraded samples.[51–53] At high pump intensities, defect states get activated via charge transfer mediated by doubly excited molecules. This results in a new defect-related PA feature, suppressing the SE. The subpicosecond buildup of a new PA band [see Fig. 9(a)] is consistent with ultrafast growth dynamics of the PA_2 feature (Fig. 8), which is generated via a similar charge-transfer mechanism.

V. CONCLUSIONS

We have performed femtosecond TA studies of a five-ring PPV oligomer (MEH-DSB) prepared in two forms: solid-state films and dilute solutions. In solutions, at low pump intensities, all of the TA features (SE and PA) are due to a single species, which we identify as singlet excitons. The decay of these species leads to wavelength-independent exponential relaxation of the TA with a time constant of 650 ps, associated with radiative processes. At high pump intensities for which a significant fraction of molecules is doubly excited, we observe deviations from a single-exponential decay for both the PA and SE features. In this pump-intensity regime, the SE decay exhibits an additional fast component with a time constant of $\sim$160 ps. The amplitude of this component grows quadratically with respect to the amplitude of the slow component, indicating the generation of two-exciton states. The shortening of the initial SE relaxation is explained in terms of enhanced radiative decay (enhanced oscillator strength) of biexcitons. The enhanced biexciton oscillator strength is also responsible for superlinear growth of the SE signal at high pump intensities. We observe increasing deviations in PA and SE dynamics with increasing the pump level, which is due to different relative exciton/biexciton contributions into these two signals. A simple model taking into account the generation of biexcitons via a sequential reexcitation of singly excited molecules allows an excellent fit of both the TA dynamics and pump dependence.

In addition to the long-wavelength PA band (PA_1) observed in solutions, film samples exhibit a short-wavelength PA feature (PA_2), which has distinct dynamics and pump dependence from those of PA_1. The matching dynamics of PA_1 and SE in pristine films over a wide pump-intensity range demonstrates unambiguously that these features originate from intrachain singlet excitons. On the other hand, the pump-independent dynamics of PA_2, along with the fact that it is only observed in solid-state samples, suggests that this feature is due to strongly correlated geminate electron-hole pairs located on adjacent chains (interchain excitons). As in solutions, we observe an additional fast component in the SE and PA_1 signals growing quadratically with the pump fluence, which we attribute to generation of two-exciton states or biexcitons. However, in films this quadratic component is extremely short lived (subpicosecond decay time), indicating that biexcitons are unstable. We observe clear correlations between the subpicosecond relaxation of the fast TA component and the buildup dynamics of the short-wavelength PA_2 band, indicating that the subpicosecond biexciton decay is due to ultrafast charge transfer accompanied by the formation of interchain species.

Additionally, we observe a strong effect of photodegradation on TA in solid-state films, manifested as an overall reduction of the TA signal and a drastic shortening of SE dynamics at high pump levels. This is explained in terms of generation of defects that contribute to TA by a negative signal spectrally overlapping with SE. Defect states can only be activated at high pump fluences via a charge-transfer process mediated by intrachain two-exciton states. Therefore, in degraded films, SE and PA_1 dynamics match each other at low pump intensity but are strongly different at high pump fluences.

ACKNOWLEDGMENTS

We thank I. Campbell for the preparation of MEH-DSB samples. This work was supported by Los Alamos National Laboratory Directed Research and Development funds under the auspices of the U.S. Department of Energy.

[1] D. W. McBranch and M. B. Sinclair, in *The Nature of the Photoexcitations in Conjugated Polymers*, edited by N. S. Sariciftci (World Scientific Publishing, Singapore, 1997).
[2] R. Kersting, U. Lemmer, R. F. Mahrt, K. Leo, H. Kurz, H. Bässler, and E. O. Göbel, Phys. Rev. Lett. **70**, 3820 (1993).
[3] I. D. W. Samuel, F. Raksi, D. D. C. Bradley, R. H. Friend, P. L. Burn, A. B. Holmes, H. Murata, T. Tsutsui, and S. Saito, Synth. Met. **55**, 15 (1993).
[4] J. M. Leng, S. Jeglinski, X. Wei, R. E. Benner, Z. V. Vardeny, F. Guo, and S. Mazumdar, Phys. Rev. Lett. **72**, 156 (1994).
[5] J. W. P. Hsu, M. Yan, T. M. Jedju, L. J. Rothberg, and B. R. Hseih, Phys. Rev. B **49**, 712 (1994).
[6] M. Yan, L. J. Rothberg, F. Papadimitrakopoulos, M. E. Galvin, and T. M. Miller, Phys. Rev. Lett. **72**, 1104 (1994).
[7] M. Yan, L. J. Rothberg, B. R. Hsieh, and R. R. Alfano, Phys. Rev. B **49**, 9419 (1994).
[8] M. Yan, L. J. Rothberg, E. W. Kwock, and T. M. Miller, Phys. Rev. Lett. **75**, 1992 (1995).
[9] W. Graupner, G. Leising, G. Lanzani, M. Nisoli, S. DeSilvestri, and U. Scherf, Phys. Rev. Lett. **76**, 847 (1996).
[10] N. T. Harrison, G. R. Hayes, R. T. Phillips, and R. H. Friend, Phys. Rev. Lett. **77**, 1881 (1996).
[11] J. W. Blatchford, S. W. Jessen, L. B. Lin, J. J. Lih, T. L. Gustafson, A. J. Epstein, D. K. Fu, M. J. Marsella, T. M. Swager, A. G. Macdiarmid, S. Yamaguchi, and H. Hamaguchi, Phys. Rev. Lett. **76**, 1513 (1996).
[12] B. J. Schwartz, F. Hide, M. R. Andersson, and A. J. Heeger, Chem. Phys. Lett. **265**, 327 (1997).
[13] E. Maniloff, V. I. Klimov, and D. W. McBranch, Phys. Rev. B **56**, 1876 (1997).
[14] S. Mukamel and H. X. Wang, Phys. Rev. Lett. **69**, 65 (1992).
[15] S. Abe, M. Schreiber, W. P. Su, and J. Yu, Phys. Rev. B **45**, 9432 (1992).
[16] R. H. Friend, D. D. C. Bradley, and P. Townsend, J. Phys. D **20**, 1367 (1987).
[17] A. J. Heeger, S. Kivelson, J. R. Schrieffer, and W.-P. Su, Rev. Mod. Phys. **60**, 781 (1988).
[18] V. Klimov, D. McBranch, N. N. Barashkov, and J. P. Ferraris, Chem. Phys. Lett. **277**, 109 (1997).
[19] S. V Frolov, W. Gellerman, M. Ozaki, K. Yoshino, and Z. V. Vardeny, Phys. Rev. Lett. **78**, 729 (1997).
[20] M. Kuwatagonokami, N. Peyghambarian, K. Meissner, B. Fluegel, Y. Sato, K. Ema, R. Shimano, S. Mazumdar, F. Guo, T. Tokohiro, H. Ezaki, and E. Hanamura, Nature (London) **367**, 47 (1994).
[21] F. Guo, M. Chandross, and S. Mazumdar, Phys. Rev. Lett. **74**, 2086 (1995).
[22] Z. G. Yu, R. T. Fu, C. Q. Wu, X. Sun, and K. Nasu, Phys. Rev. B **52**, 4849 (1995).
[23] F. B. Gallagher and F. C. Spano, Phys. Rev. B **53**, 3790 (1996).
[24] S. Mazumdar, F. Guo, K. Meissner, B. Fluegel, N. Peyghambarian, M. Kuwatagonokami, Y. Sato, K. Ema, R. Shimano, T. Tokohiro, H. Ezaki, and E. Hanamura, J. Chem. Phys. **104**, 9292 (1996).
[25] V. Klimov, D. McBranch, N. N. Barashkov, and J. P. Ferraris, Proc. SPIE **3145**, 58 (1997).
[26] G. Kranzelbinder, W. Graupner, K. Mullen, U. Scherf, and G. Leising, Proc. SPIE **3145**, 48 (1997).
[27] G. Klein, C. Jundt, B. Sipp, A. A. Villaeys, A. Boeglin, A. Yassar, G. Horowitz, and F. Garnier, Chem. Phys. **215**, 131 (1997).
[28] M. Chandross, Y. Shimoi, and S. Mazumdar, Chem. Phys. Lett. **280**, 85 (1997).
[29] G. Kranzelbinder, M. Nisoli, S. Stagira, S. Desilvestri, G. Lanzani, K. Mullen, U. Schert, W. Graupner, and G. Leising, Appl. Phys. Lett. **71**, 2725 (1997).
[30] O. Akimoto and E. Hanamura, Solid State Commun. **10**, 253 (1972).
[31] E. Hanamura, Solid State Commun. **12**, 951 (1973).
[32] K. Misawa, H. Yao, T. Hayashi, and T. Kobayashi, J. Cryst. Growth **117**, 617 (1992).
[33] S. Shionoya, H. Saito, E. Hanamura, and O. Akimoto, Solid State Commun. **12**, 223 (1972).
[34] A. Mysyrowicz, J. B. Grun, R. Levy, A. Bivas, and S. Nikitine, Phys. Lett. **26A**, 615 (1968).
[35] C. H. Henry and K. Hassau, J. Lumin. **1&2**, 299 (1970).
[36] Y. Z. Hu, S. W. Koch, and D. B. Tran Thoai, Mod. Phys. Lett. B **4**, 1009 (1990).
[37] V. Klimov, S. Hunsche, and H. Kurz, Phys. Rev. B **50**, 8110 (1994).
[38] A. Dogariu, D. Vacar, and A. J. Heeger, Chem. Phys. Lett. **290**, 587 (1998).
[39] M. D. Joswick, I. H. Campbell, N. N Barashkov, and J. P. Ferraris, J. Appl. Phys. **80**, 2883 (1996).
[40] M. Fahlman, M. Logdlund, S. Stafstrom, W. R. Salaneck, R. H. Friend, P. L. Burn, and A. B. Holmes, Macromolecules **28**, 1959 (1995).
[41] B. E. Kohler and I. D. W. Samuel, J. Chem. Phys. **103**, 6248 (1995).
[42] J. Cornil, D. Beljonne, Z. Shuai, T. W. Hagler, I. Campbell, D. D. C. Bradley, J. L. Bredas, C. W. Spangler, and K. Mullen, Chem. Phys. Lett. **247**, 425 (1995).
[43] V. I. Klimov and D. W. McBranch, Opt. Lett. **23**, 277 (1998).
[44] D. Moses, Appl. Phys. Lett. **60**, 3215 (1992).
[45] L. Smilowitz, A. Hays, A. J. Heeger, G. Wang, and J. E. Bowers, J. Chem. Phys. **98**, 6504 (1993).
[46] N. Tessler, G. J. Denton, and R. H. Friend, Nature (London) **382**, 695 (1996).
[47] F. Hide, M. A. DiazGarcia, B. J. Schwartz, M. R. Andersson, Q. B. Pei, and A. J. Heeger, Science **273**, 1833 (1996).
[48] L. J. Rothberg, F. Papadimitrakopoulos, and M. Galvin, Synth. Met. **80**, 41 (1996).
[49] G. S. Kanner, X. Wei, B. C. Hess, L. R. Chen, and Z. V. Vardeny, Phys. Rev. Lett. **69**, 538 (1992).
[50] G. J. Denton, N. Tessler, N. T. Harrison, and R. H. Friend, Phys. Rev. Lett. **78**, 733 (1997).
[51] M. Yan, L. J. Rothberg, F. Papadimitrakopoulos, M. E. Galvin, and T. M. Miller, Phys. Rev. Lett. **73**, 744 (1994).
[52] D. G. J. Sutherland, J. A. Carlisle, P. Elliker, G. Fox, T. W. Hagler, I. Jimenez, H. W. Lee, K. Pakbaz, L. J. Terminello, S. C. Williams, F. J. Himpsel, D. K. Shuh, W. M. Tong, J. J. Jia, T. A. Calcott, and D. L. Ederer, Appl. Phys. Lett. **68**, 2046 (1996).
[53] G. Yu, J. Gao, J. C. Hummelen, F. Wudl, and A. J. Heeger, Science **270**, 1789 (1995).